

Extended Modified Liquid Drop–Dynamical Nucleation Theory (EMLD–DNT) Approach to Nucleation: A New Theory[†]

David Reguera* and Howard Reiss

Department of Chemistry and Biochemistry, University of California at Los Angeles (UCLA),
607 Charles E. Young Drive East, Los Angeles, California 90095

Received: June 29, 2004; In Final Form: August 20, 2004

We present a new phenomenological approach to nucleation, based on the combination of the “extended modified liquid drop” (EMLD) model and dynamical nucleation theory (DNT). The new model proposes a new cluster definition, which properly includes the effect of fluctuations, and it is consistent both thermodynamically and kinetically. The model is able to predict successfully the free energy of formation of the critical nucleus, using only macroscopic thermodynamic properties. The nucleation barrier predicted by the model vanishes at a finite value of the supersaturation, thus accounting for the spinodal, and provides excellent agreement with the results of recent simulations. Of fundamental importance is the fact that the cluster definition is based on cluster volume as well as molecular content, and that a nonarbitrary specification of volume is supplied by variational transition state theory. In this connection, the importance of allowing the “process” to define the cluster is demonstrated. This nexus between chemical dynamics and nucleation should lead to a collaboration of nucleation theorists and chemical dynamicists that will form a whole that is greater than the sum of its parts.

1. Introduction

Nucleation is the first step in many phase transformations and has a very important role in many areas of science and technology, ranging from biophysics to atmospheric science. Despite this multidisciplinary impact, it still is not a well-understood phenomenon. The main reason lies in the special features of the phenomenon, intrinsically a nonequilibrium process, where the most important entity, the critical cluster or “nucleus”, is unstable and typically contains only a few molecules. This thermodynamically unstable character makes it hard to evaluate nucleus properties by either experiment or simulation. In addition, its molecular nature casts doubt on the validity of extrapolating standard well-known theories down to the nanoscale.

The optimal way to tackle this problem would seem to be the development of a fully kinetic molecular theory, focused on the nonequilibrium nature of the phenomenon and based on the definition of a cluster at the molecular scale, together with knowledge of intermolecular potentials.¹ However, this task is complicated by the lack of accurate potentials for most substances and difficulties in the identification, and even in the definition, of a physically consistent cluster. Unfortunately, the results of molecular theories are very sensitive to the accuracy of both features.

The relative success of recent approaches, such as “density functional theory” (DFT),^{2,3} have not succeeded in supplanting “classical nucleation theory” (CNT),^{4–6} which is still the most commonly used framework for describing nucleation. Despite its shortcomings, CNT is a very simple theory and provides reasonable estimates of the magnitudes of nucleation rates based

only on experimentally accessible information such as the (bulk) values of density, vapor pressure, and (planar) surface tension. However, in some cases, the predictions of CNT are in severe disagreement with experiment. A more serious flaw of CNT is the fact that it is unable to predict a spinodal.

Because of the above-mentioned difficulties in developing molecular approaches, phenomenological models are still desirable and have been intensely pursued. These have included the use of the Fisher droplet model⁷ and its variants,^{8,9} corrections to the height of the nucleation barrier to force it to vanish at the spinodal, based on scaling arguments,¹⁰ and especially the application of different assumptions concerning the choice of droplet dividing surface or surface tension.^{11–13} However, the proposed modifications of CNT have either not succeeded in improving the predictions of CNT or have required information that is not easily available.

In this paper, we present a promising new phenomenological model for nucleation, based on a combination of the “extended modified liquid drop model” (EMLD)^{14,15} and “dynamical nucleation theory” (DNT).¹⁶ This model does not require information about the intermolecular potentials but, instead, using the same macroscopically measurable parameters as CNT, is able to predict the spinodal. Moreover, it provides very good agreement with recent simulations of nucleation in Lennard-Jones systems¹⁷ and also satisfies recently proposed scaling relations.¹⁸ It also provides an important connection between kinetic molecular approaches and equilibrium approaches, based on the evaluation of the free energy of cluster formation. In so doing, it offers the promise of bringing together chemical dynamicists and nucleation theorists, to form a whole that is greater than the sum of its parts.

The paper is arranged as follows. In section 2, the main features of the EMLD model are reviewed. In section 3, EMLD is combined with DNT to yield a new model for nucleation, which, unlike CNT, predicts the spinodal. Results for vapor-

[†] Part of the special issue “Frank H. Stillinger Festschrift”.

* Author to whom correspondence should be addressed. Present address: Universitat de Barcelona, Departament de Física Fonamental, Martí i Franqués, 1, Barcelona 08018, Spain. E-mail: dreguera@ub.edu.

phase nucleation of an almost-ideal gas are reported in section 4. In section 5, we extend the model to treat nonideal systems and compare its predictions with the simulation results of Ten Wolde and Frenkel¹⁷ on nucleation in a Lennard-Jones fluid. In section 6, the temperature dependence of the nucleation rates that is predicted by the model is analyzed. Finally, a critical discussion of the model, along with its main conclusions, are presented in sections 7 and 8.

2. The Extended Modified Liquid Drop Model (EMLD)

We begin by describing the recently developed EMLD model.^{14,15} This model was able to reproduce, with remarkable accuracy, the simulated properties of very small confined systems, which contained just a few molecules. It was used to study the behavior of a very small “canonical” system of N molecules confined to a spherical container of volume V and radius R , at temperature T . Under appropriate conditions, a liquid drop could form inside the container at any position that did not require it to be deformed. The drop itself, which is modeled according to the “capillarity approximation” (incompressible, sharp interface with the vapor, uniform density and surface tension equal to that of the bulk liquid), is assumed to contain n molecules and be surrounded by an ideal gas, constituted by the remaining $N - n$ molecules (although the ideality of the vapor phase is not an essential requirement and will, in fact, be relinquished later). For the system as described, the Helmholtz free energy of formation $\Delta F(n)$ of the drop containing n molecules, at a fixed position within the container, can be evaluated by thermodynamic means alone, yielding¹⁴

$$\Delta F(n) = -nkT \ln \left(\frac{p_1}{p_{\text{eq}}} \right) + \sigma A + n(kT - v_l p_{\text{eq}}) + NkT \ln \left(\frac{p_1}{p_0} \right) \quad (1)$$

where p_1 is the pressure exerted by the ideal gas ($p_1 = (N - n)kT/(V - v_l n)$), p_{eq} is the vapor pressure of the bulk liquid, σ is the (planar) surface tension, A is the surface area of the spherical drop of radius r containing n molecules, v_l is the volume per molecule in the liquid, and $p_0 = NkT/V$. In eq 1, the first term on the right is the usual bulk term related to the supersaturation (although, in this case, the supersaturation is not fixed), the second term accounts for the contribution of the surface, the third term is the volume work (usually small and commonly neglected), and the last term has its origin in the depletion of vapor molecules when a drop is formed. In the thermodynamic limit, $p_1 = p_0$ and the CNT expression for the free energy is recovered.

For very small systems, i.e., systems containing just a few molecules, there are some corrections, which are neglected in macroscopic thermodynamics, that become very important. In the EMLD model,¹⁴ two such contributions are incorporated. These are (i) the translation of the drop through the volume of the container, and (ii) the effect of fluctuations in n , the molecular content of the cluster. In regard to contribution (i), the drop is not necessarily required to appear precisely at the center of the container; it can collide with the walls, thus contributing to the total pressure $p(n)$ in the container. The pressure $p(n)$ then consists of the sum of the gas pressure p_1 and the pressure p_{drop} exerted by the translating drop, which is regarded as a single ideal hard sphere molecule, i.e.,

$$p(n) = p_1(n) + \frac{kT}{(4\pi/3)(R - r)^3} \Theta(n) \quad (2)$$

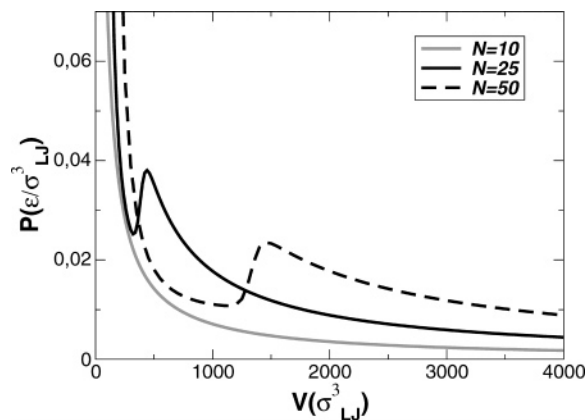


Figure 1. Pressure–volume (P – V) isotherms for Lennard-Jones argon at $T = 85$ K and different values of N . The values of the surface tension, liquid density, and equilibrium vapor pressure are the same as in ref 14.

where $4\pi(R - r)^3/3$ is the volume through which the center of the drop can translate, and $\Theta(n)$ is the unit step function that accounts for the fact that this translational contribution must be considered only when the drop is present. For contribution (ii), although N , V , and T are held constant, the number n of molecules in the drop can fluctuate, so that the chance of having a drop of size n is given by¹⁹

$$f(n) = \frac{e^{-\Delta F(n)/(kT)}}{\sum_{j=0}^N e^{-\Delta F(j)/(kT)}} \quad (3)$$

Clearly, such fluctuations are only important in very small systems. Nevertheless, thermodynamically consistent properties should be obtained as averages using $f(n)$ as a weight function. In particular, the pressure should be obtained by averaging $p(n)$ in eq 2 as

$$P = \langle p(n) \rangle = \sum_{n=0}^N f(n) \left[p_1(n) + \frac{kT}{(4\pi/3)(R - r)^3} \Theta(n) \right] \quad (4)$$

The exception to this rule is, of course, the total Helmholtz free energy, which should be calculated through the standard expression

$$\Delta F = -kT \ln \left(\sum_{n=0}^N e^{-\Delta F(n)/(kT)} \right) \quad (5)$$

Pressure–volume (P – V) isotherms predicted by the EMLD model for systems that contain Lennard-Jones (LJ) argon with different molecular contents N , at $T = 85$ K, are plotted in Figure 1. For large N , the isotherms have a van der Waals looplike shape, whose origin can be physically explained. Thus, for very small volumes, almost all molecules are condensed to a drop, leaving just a few vapor molecules tightly squeezed between the drop and the boundary of the volume. As the volume increases, the pressure initially decreases, because the evaporation due to the increase of V does not introduce enough molecules into the vapor phase to increase the vapor density. This situation continues until a minimum pressure is reached at a volume V_{min} . At this point, the evaporation of the drop becomes dominant and increases the number of vapor molecules, relative to a continued volume increase, resulting in an increase of vapor density and a corresponding increase in pressure. If

the volume continues to be increased, a point is reached where the pressure of the vapor cannot equal the equilibrium pressure of the diminishing evaporating drop anymore, so it evaporates completely, leaving only gas (modeled here as ideal) and its corresponding pressure in the container. However, the behavior of the P – V isotherms becomes very different for very small values of N . Below a certain N , in this case, in the neighborhood of $N = 15$ for the system and conditions of Figure 1, the loop in the isotherm disappears due to the effect of fluctuations, and the P – V isotherm simply exhibits a monotonic decrease of pressure with volume. Later, we shall see the relation of this phenomenon to the occurrence to the spinodal.

The isotherms in Figure 1 display a remarkable agreement with those generated by means of Monte Carlo (MC) simulations, regarded as experimental measurements. This agreement, for both simple and binary Lennard-Jones fluids, can be viewed in refs 14 and 15, where abundant additional discussion of the EMLD model can be found. Furthermore, in ref 20, a reasonable explanation of this agreement is presented.

It is worth reiterating that the model requires an input of only macroscopically observable properties and, thus, in essence, uses the same ingredients as CNT. However, the key feature of the EMLD model is the proper accounting for the effects of fluctuations and translation, which are very important in small systems. This is also demonstrated by the fact that the omission of these effects reduces the model to that of CNT.

The excellent accuracy achieved by the EMLD model in the description of a canonical system then becomes the basis of the formulation of a new successful model for nucleation: the EMLD–DNT model, which is described in the next section.

3. Application of EMLD to Nucleation: Cluster Volume and EMLD–DNT

In the EMLD model, emphasis was placed on the behavior of strongly confined systems, of interest, for example, on capillary condensation. However, although it is relatively easy to see how the model can represent a fluid undergoing capillary condensation in a nanopore (the container being representative of the pore), it is not clear immediately how it might be used in nucleation theory. A first difficulty is that the canonical ensemble is obviously not the most relevant one for nucleation, a process that typically occurs under controlled pressure or chemical potential. In addition, the definition of the cluster relevant to nucleation is not obvious on an a priori basis.

The original motivation underlying the “modified liquid drop” (MLD) model²¹ was the use of the canonical system, *as a whole*, as the cluster. Following this spirit of MLD, the new model is based on the assumption that the (N, V, T) system described by the EMLD also becomes, *as a whole*, the “physical” cluster for nucleation. It will be demonstrated in this section that this assumption is not only thermodynamically consistent, but also the proper definition, from the dynamical point of view.

Notice that this (N, V, T) system, as a whole, constitutes a “diffuse” cluster that includes some vapor and differs from the compact capillary cluster of CNT by the presence of the volume V as a second defining variable. In fact, in ref 14, we showed that the EMLD clusters have smooth density profiles, even though they are constructed from a sharp capillarity profile. The necessity of including the volume as a relevant variable in the description of a physical cluster was already noted by molecular theories developed by Reiss and co-workers, who introduced the (i, v) -cluster.^{21–24} However, the main problem in this development was the absence of a nonarbitrary physical criterion for selecting the volume of the cluster. This situation

was aggravated by the relative insensitivity to volume, in some ranges, of the cluster free energy.²⁵ However, there are strong arguments, both from thermodynamics and kinetics, that support the notion that the volume V_{\min} corresponding to the minimum of a P – V isotherm, such as those of Figure 1, is the appropriate cluster volume.

Thermodynamically, some excellent insight concerning the choice of V was supplied in an important work of Talanquer and Oxtoby on the development of DFT in the canonical ensemble.²⁶ In their work, the properties of Lennard-Jones (i, v) -clusters were evaluated by means of DFT. In essence, the system consisted of i molecules confined to a spherical container of volume V , and was therefore closely related to the spherical system addressed by the EMLD model (although the latter system did not use an intermolecular potential, whereas, to expedite the application of DFT, the former one did). Using a mean field free-energy functional, these authors were able to evaluate, among other things, the P – V isotherms and construct the two-dimensional free-energy landscape for the formation of these (i, v) -clusters. As indicated previously, for sufficiently small volumes, a drop can form in the system, and DFT predicts nonuniform profiles, resembling a liquid core surrounded by vapor. However, Talanquer and Oxtoby noticed that sets of clusters could be found, such that the liquid cores were equivalent both in size and appearance. The only difference among these systems was that they contained different amounts of vapor. Based on this observation, they proposed the idea (similar to that suggested by Reiss²⁷) that a core formed inside the container has an intrinsic structure, whose nature is mainly determined by the interaction among the molecules forming it, and is relatively insensitive to the vapor surrounding it. Therefore, they reasoned that the members of a set of (i, v) -clusters exhibiting similar cores, were, in a sense, redundant, so that only one of them, which they called a *stable i-cluster*, was physically relevant. The structure of the two-dimensional (N, V) free energy landscape made it reasonable to identify this cluster as the member of the set that contained the smallest amount of “vapor”. Using N in place of i , this meant that, for a given N , the *stable N-cluster* was the one exerting the lowest pressure. For a given N , this requirement is fulfilled at the minimum of the P – V isotherm for that N , and, hence, the volume of the stable N -cluster was chosen as the volume corresponding to this minimum ($V = V_{\min}$). Further details are available in ref 26.

Another independent criterion for the selection of the volume comes from kinetic considerations that involve dynamical nucleation theory (DNT).¹⁶ Nucleation is essentially a kinetic process; thus, any meaningful definition of a cluster, valid for nucleation, must also refer to kinetics. It is then reasonable to search in the theory of rate processes for a physical criterion for the value of V , because the phenomenon may be regarded as a chemical process in which single molecules are reactants and clusters are products. From this point of view, the definition of a cluster should relate to the kinetics of the addition and the loss of cluster molecules. This is the view adopted in the pioneering work of Garrett and co-workers in their development of DNT.¹⁶

In DNT, a cluster is defined as a collection of N molecules confined within an arbitrary spherical dividing surface of radius R and volume V . In the language of DNT, the spherical boundary of the cluster is the reaction surface that separates reactants (the cluster) from products, and the evaporation of the cluster is regarded as the reaction. Using transition-state theory (TST), the rate of evaporation can be shown to be proportional to the

derivative, with respect to R , of the Helmholtz free energy of the cluster and, in units of molecules per second, is given by

$$\alpha_N^{\text{TST}} = - \left(\frac{1}{2\pi m k T} \right)^{1/2} \frac{dF(N, T, R)}{dR} = \frac{\bar{c}}{4} (4\pi R^2) \frac{P_{\text{int}}}{kT} \quad (6)$$

in which m is the molecular mass, \bar{c} is the average speed of the molecules in the gas phase ($\bar{c} = [8 kT/(\pi m)]^{1/2}$), $P_{\text{int}} = -dF(N, T, R)/dV$, and $V = 4\pi R^3/3$. The TST approximation to the flux through the dividing surface is an upper bound to the exact classical reactive flux, because, among other things, it does not take into account possible recrossings of the barrier. This upper bound is the basis for variational transition-state theory (VTST),²⁸ in which the location of the dividing surface (or the radius of the volume of the cluster in our case) is chosen to minimize the reactive flux. In the original formulation of DNT, the reactive flux to be minimized was given by

$$q^R(N, T, R_{\text{opt}}) \alpha_N^{\text{VTST}}(T) = \min_R \left\{ \frac{kT}{h} q^{\text{GT}}(N, T, R) \right\} \quad (7)$$

where $q^R(N, T, R_{\text{opt}})$ is the partition function of the reactant (the cluster), $q^{\text{GT}}(N, T, R)$ the partition function of the system in the transition state, and R_{opt} the radius of the cluster that minimizes the reactive flux. In ref 16, the transition-state partition function was evaluated and yielded a VTST rate constant:

$$\begin{aligned} \alpha_i^{\text{VTST}} &= - \left(\frac{1}{2\pi m k T} \right)^{1/2} \frac{dF(N, T, R_{\text{opt}})}{dR} \\ &= \frac{\bar{c}}{4} (4\pi R_{\text{opt}}^2) \frac{P_{\text{int}}(R_{\text{opt}})}{kT} \end{aligned} \quad (8)$$

Consequently, DNT, or more precisely VTST, shows that the proper kinetic definition of the volume of a cluster is tied to the minimization of its evaporation rate.

However, there are some subtle differences between the original formulation of DNT and the application of the concepts of DNT to our model, and these differences are worth stressing. First, in the original formulation of DNT, the center of the spherical dividing surface was chosen to coincide with the cluster center of mass. This choice was selected for simplicity, although, as the authors indicated later,²⁹ other definitions could be used. In particular, in EMLD–DNT, we use a different definition of the dividing surface such that the center of the mass of the EMLD cluster is not forced to lie at the center of the container. Second, there is, apparently, a small ambiguity in the quantity that should be minimized in VTST. For example, the reactive flux, the reaction constant, the reaction flux per unit volume, the activation free energy, or even the density of states are different quantities chosen for minimization in different versions of VTST. For instance, in the original DNT, the reactive flux defined by eq 7, was the quantity minimized in obtaining the optimum radius R_{opt} . Generally, this differs mathematically, from the requirement of minimum pressure. However, if the quantity minimized is the evaporation flux, defined as the rate of evaporation per unit surface area of the cluster, i.e., $\alpha_N^{\text{TST}}/(4\pi R^2)$, then eq 8 shows that this requirement for a cluster of N molecules is realized by selecting the volume that minimizes the pressure P_{int} and, hence, reduces to exactly the choice suggested by Talanquer and Oxtoby. Thus, in this case, the thermodynamic and the kinetic criteria coincide and choose, for the volume of an N -cluster, V_{min} , the volume at the minimum of the corresponding P – V isotherm.

Still, another physical argument supports this selection of the volume. In some versions of VTST, the dividing surface is chosen as the one that minimizes the reversible work required to displace it by a small amount. In our case, the reversible work involved in shifting the location of the dividing surface (defined in terms of cluster volume) by dV is just pressure–volume work, and the minimum reversible work is accomplished at the cluster volume that minimizes the pressure, i.e., at the volume corresponding to the minimum of the isotherm. In some cases, the free energy of the transition state is minimized. Note that the selection criterion does not seem to be very unique. However, different choices seem to result in only small differences in the predicted rate constant.

As a result of the foregoing, we will denote the volume to be used in defining our EMLD–DNT cluster (i.e., the volume at the isotherm minimum) as $V_{\text{min}}(N)$.

Now, the value of V_{min} can be obtained numerically as the minimum, $\partial P/\partial V|_{V_{\text{min}}} = 0$, of P in eq 4. We have also verified that a very good approximation to V_{min} can be obtained following a simpler route. As mentioned previously, the minimum of the P – V isotherm marks the physical onset of evaporation of the drop, and this onset corresponds to the volume for which the stable drop of EMLD (minimum of $[\Delta F(n)]_{N, V, T}$, with respect to n), becomes metastable. Therefore, a very good approximation to V_{min} can be obtained from the simultaneous solution of $[\partial(\Delta F)/\partial n]_{N, V, T} = 0$ and $[\Delta F(n_{\text{drop}})]_{N, V, T} = 0$, equations which define the EMLD stable drop and the onset of metastability, respectively.

After the volume of the EMLD–DNT cluster has been specified, the next step involves the use of eq 5, which represents the EMLD prediction for the Helmholtz free energy of the entire N, V_{min}, T system. This value can be used to construct the work of formation of the new physical EMLD–DNT cluster in the open μ, V, T system, which is the relevant ensemble for nucleation. It can be proved, both from thermodynamics³⁰ or from statistical mechanics, that at a chemical potential μ and pressure p , the Gibbs free energy of cluster formation or a demonstrable equivalent change in the grand potential of cluster formation, are related to the corresponding Helmholtz free energy of formation as follows:

$$(\Delta G)_{N, p, T} = (\Delta \Omega)_{\mu, V_{\text{min}}, T} = (\Delta F)_{N, V_{\text{min}}, T} - V_{\text{min}} \Delta p + N \Delta \mu_0 \quad (9)$$

for $\Delta p = p_0 - p$ and $\Delta \mu_0 = \mu_0 - \mu$, where μ_0 is the value of the chemical potential of a uniform vapor of pressure p_0 , at the uniform density $\bar{\rho}$ ($\bar{\rho} = N/V$), and μ and p are the externally imposed values of the chemical potential and pressure. The general proof of eq 9 is somewhat subtle, so we provide a derivation and some clarification in the Appendix. In the Appendix, p_0 is represented by $p(\bar{\rho})$ and μ_0 is represented by $\mu(\bar{\rho})$.

Although N is the natural size variable for the model, it is worth stressing that it does not represent the physically relevant quantity for a nucleation cluster. Instead, the so-called “molecular excess” serves as the relevant quantity. This is another important difference from the original DNT, formulated using N as the size of the cluster. As we shall see later, the molecular content of an EMLD–DNT cluster is defined in terms of the excess given by the “nucleation theorem”.^{31,32}

Equation 9 provides the Gibbs free energy of formation of an EMLD–DNT cluster of fixed size N for arbitrary values of chemical potential or supersaturation, or, for a fixed μ , the values of the work of formation of clusters of different sizes N . However, for nucleation, the most important quantity is the

height of the nucleation barrier, i.e., the free energy of formation of the critical cluster or nucleus. This can also be obtained from eq 9 under special conditions (see Appendix). Generally, the size N^* of the critical cluster and the height ΔG^* of the nucleation barrier are obtained from the condition $[\partial(\Delta G)_{N,p,T}/\partial N]_{V,T|N=N^*} = 0$. By imposing this condition on eq 9, one finds (see Appendix)

$$\left[\frac{\partial(\Delta F)_{N,V,T}}{\partial N} \right]_{V_{\min},T|N=N^*} = -\Delta\mu_0 = \mu - \mu_0 \quad (10)$$

which is immediately satisfied when the value of N (and its corresponding V_{\min}) is such that the chemical potential of the N, V_{\min} cluster (and its corresponding pressure) is equal to the externally imposed chemical potential μ (or pressure p) (see Appendix). This also means that each N -cluster can serve as a critical nucleus at some appropriate chemical potential (or supersaturation). In that case, eq 9 still gives the height of the appropriate nucleation barrier in both the constant pressure and constant μ ensembles, i.e.,

$$(\Delta G^*)_{N,p,T} = (\Delta\Omega^*)_{\mu,V,T} = [\Delta F(N^*, V_{\min})]_{N,V,T} - V_{\min}(p_0 - P^*) + N^*\Delta\mu_0^* \quad (11)$$

where $\Delta F(N^*, V_{\min})$ is given by eq 5, V_{\min} is the volume corresponding to the minimum of the P – V isotherm for each value of N^* , P^* is the average value of the pressure given by eq 4, and, for an ideal vapor, $\Delta\mu_0^* = k_B T \ln(p_0/P^*)$. Equation 11 is the work of formation of the critical cluster, rendered physically significant through the use of the nonarbitrary cluster volume, and constitutes the main result of the EMLD–DNT model for nucleation.

There is also a more-physical justification of the procedure just described for obtaining the height of the nucleation barrier, advanced in the work of Talanquer and Oxtoby.²⁶ Each value of N^* , T , and the corresponding V_{\min} , defines the pressure and the chemical potential of an EMLD–DNT cluster, which is a diffuse entity and contains some amounts of vapor. If this cluster is now immersed in a homogeneous vapor that has the same chemical potential and pressure as the EMLD–DNT cluster, and the boundary of the container is somehow removed, we would have the EMLD–DNT cluster coexisting (in *unstable* equilibrium) with the vapor. However, in an open system, only an unstable cluster can be in “thermodynamic” coexistence with the vapor, namely, the critical cluster or nucleus. Therefore, if the external vapor has both a pressure and chemical potential equal to those of the EMLD–DNT cluster, this cluster serves as the critical cluster for this value of the supersaturation.²⁶

Results of the application of the EMLD–DNT model are reported in the following sections.

4. EMLD–DNT for Ideal Systems

For simplicity, we first report the predictions of the EMLD–DNT model for the case in which the nucleating vapor behaves approximately as an ideal gas. In the next section, nonideal systems are addressed.

Equation 11 provides the height of the Gibbs free energy of formation of the critical cluster. In the case where the nucleating vapor behaves as an ideal gas, we have the following conditions: $p_0 = N^*kT/V_{\min}$ and $\Delta\mu_0^* = kT \ln(p_0/P^*)$. Operationally, the calculation of the height of the nucleation barrier is as follows. For a given value of N^* , we find the optimum volume V_{\min} , by locating (numerically) the minimum of the P – V isotherm given by eq 4. The pressure P^* of the (N^*, V_{\min}) cluster,

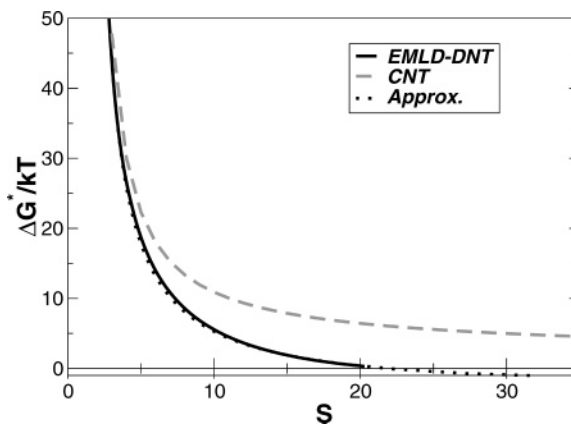


Figure 2. Gibbs free energy of formation of the critical cluster as a function of the saturation ratio S for ideal argon at $T = 85$ K using the EMLD–DNT model (heavy line) and classical nucleation theory (CNT, dashed line). The dotted line represent the values of the nucleation barrier obtained using the approximation described in the main text.

the corresponding chemical potential difference ($\Delta\mu_0^* = k_B T \ln(p_0/P^*)$), and the Helmholtz free energy ($\Delta F(N^*, V_{\min}, T)$), given by eq 5) then are substituted into eq 11 to yield the height of the barrier, for the saturation ratio $S = P^*/p_{\text{eq}}$. By repeating this procedure for different values of N^* , one obtains the nucleation barrier for different values of supersaturation.

The results for Lennard-Jones argon at $T = 85$ K (whose vapor phase is approximated as ideal) are plotted in Figure 2 and compared with the predictions of CNT:

$$\Delta G_{\text{CNT}}^* = \frac{16\pi}{3} \left[\frac{v_l^2 \sigma^3}{(kT \ln S)^2} \right] \quad (12)$$

As indicated previously, the most impressive feature of Figure 2—and, therefore, of the new model—is the occurrence of the signature of the spinodal, i.e., the vanishing of the nucleation barrier at a sufficiently high supersaturation. In contrast, CNT predicts a finite value of the nucleation barrier for all values of supersaturation. The vanishing of the nucleation barrier is related to, and coincides with the fact that, as noted previously, for very small values of N , the P – V isotherm has no minimum! (See Figure 1.) It is worth stressing that this new feature originates in the proper inclusion of both translational effects and fluctuations in the theory. Without both ingredients, eqs 9 and 11 would reproduce the standard CNT result. Fluctuations are especially important in generating the spinodal, because, in their absence, the P – V isotherms would exhibit minima for all values of N .

An interesting comparison to perform is whether the vanishing of the nucleation barrier predicted by the EMLD–DNT theory coincides with the mean-field spinodal that is determined and defined by the equation of state. It is not obvious a priori that the location of both points should coincide accurately, because in the definition of a physical cluster of interest for nucleation, both kinetic considerations and fluctuations are involved: these are concepts that are probably not taken into consideration in the mean field spinodal obtained from the equation of state. In our case, using the Lennard-Jones equation of state of ref 33, for a reduced temperature of $T^* = 0.71$ (corresponding to $T = 85$ K for the parameters of argon), the mean field spinodal occurs at a saturation ratio of $S = 11.6$, which is different from the value at which the nucleation barrier becomes zero in Figure 2 ($S \approx 20$). The discrepancy is also likely due to the limited validity of the equation of state in the spinodal regime.

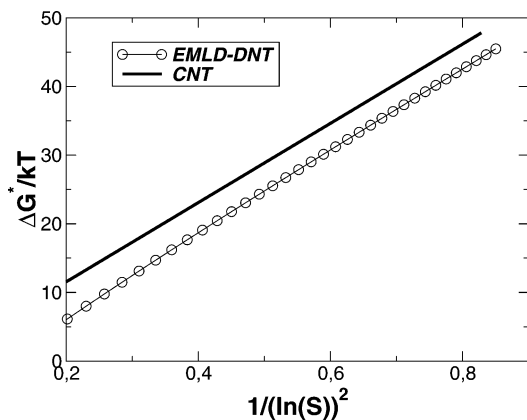


Figure 3. Height of the nucleation barrier, as predicted by the EMLD–DNT model (circles and thin line) and CNT (heavy line), as a function of $1/(\ln S)^2$, for ideal argon vapor at $T = 85$ K.

The dotted line in Figure 2 represents the predictions for the height of the Gibbs free-energy barrier that is obtained when the value of V_{\min} is located approximately by using the conditions $[\partial(\Delta F)/\partial n]_{N,V,T} = 0$ and $[\Delta F(n_{\text{drop}})]_{N,V,T} = 0$. Although these conditions have a solution for all values of N (even for $N < 15$, where the P – V isotherms of Figure 1 exhibit no minima), notice that the height of the nucleation barrier is practically zero for supersaturations beyond that corresponding to the spinodal. Consequently, the approximation is sufficiently accurate and does not provide unrealistic results, even for the range of conditions where there is no minimum in the P – V isotherms.

Another stringent test of the accuracy of the EMLD–DNT theory is whether its results scale properly. Recently, McGraw and Laaksonen¹⁸ proposed a set of scaling relations for nucleation that seem to be obeyed by most simulations and experimental data. Essentially, these relations assume that the size of the critical nucleus is correctly estimated by CNT; however, they predict a constant offset between the actual nucleation barrier and the estimates of CNT. Figure 3 plots the value of the nucleation barrier for the (ideal) Lennard-Jones system as a function of $1/(\ln S)^2$ for both the EMLD–DNT and CNT. The slopes are the same, and the values of the nucleation barrier differ only by a constant offset, showing that the EMLD–DNT model also fulfills these scaling relations.

As mentioned previously, although N^* (the total number of molecules in the EMLD–DNT cluster) is a variable that characterizes the size of the physical critical cluster, it does not represent the truly relevant quantity for nucleation, which is the molecular excess Δn^* (the excess number of molecules, with respect to the vapor phase). The Δn^* value associated with the EMLD–DNT cluster can be properly obtained in terms of the “nucleation theorem”:^{31,32}

$$\left. \frac{\partial(\Delta G^*)_{N,p,T}}{\partial \Delta \mu} \right|_{V_{\min},T} = -\Delta n^* \quad (13)$$

Therefore, the Δn^* value of an (N^*, V_{\min}) EMLD–DNT cluster can be obtained directly from the derivative of work of formation $(\Delta G^*)_{N,p,T}$, as given by eq 11, with respect to the chemical potential difference $\Delta \mu$.

In CNT, the size of the critical cluster is given by

$$n_{\text{CNT}}^* = \frac{32\pi}{3} \left[\frac{v_1^2 \sigma^3}{(KT \ln S)^3} \right] \quad (14)$$

and the expectation based on the scaling relations is that the

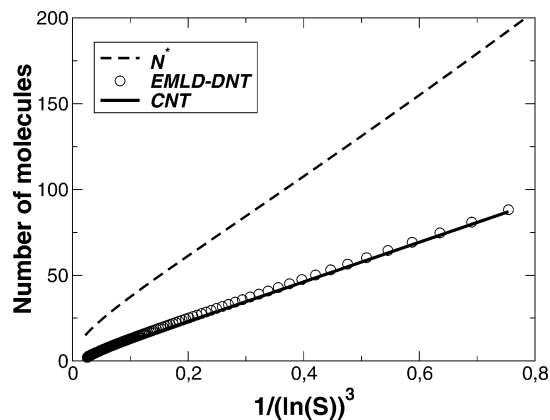


Figure 4. Number of molecules in the critical cluster (Δn^*), as a function of $1/(\ln S)^3$ for ideal argon vapor at $T = 85$ K, as predicted by the nucleation theorem in eq 13 for the EMLD–DNT (open circles) and by CNT (eq 14, heavy line). The total number of molecules (N^*) confined in the volume V_{\min} in the EMLD–DNT cluster is also plotted, for comparison.

value of the molecular excess of the critical cluster is correctly predicted by CNT.

Figure 4 plots the molecular excess, for ideal argon, of the critical nucleus (Δn^*) as a function of $1/(\ln S)^3$ for CNT, and for EMLD–DNT. The agreement between the two is remarkable, confirming the validity of EMLD–DNT and its compliance with the scaling expectations. For comparison, the different values of N^* used in the evaluation of $(\Delta G^*)_{N,p,T}$, corresponding to different values of supersaturation, are also plotted in Figure 4. From this figure, it is clear that the number of molecules in the critical (N^*, V_{\min}) -cluster generally is very different from the molecular excess of that cluster. This shows that the EMLD–DNT cluster is a “diffuse” physical entity that still contains a significant number of vaporlike molecules.

5. EMLD–DNT for Real Fluids

The application of EMLD–DNT to real (nonideal) fluids is reported in this section. The assumption that the vapor is ideal can be abandoned if the equation of state of the fluid is known. In that case, the modifications required in the EMLD–DNT model are simple. For a nonideal fluid, the pressure $P(\rho)$ is obtained directly from the equation of state, and the chemical potential can be obtained from the standard thermodynamic relation:

$$\mu_v(P) = \int_{P_{\text{eq}}}^P \frac{1}{\rho(P')} dP' + \mu_v(p_{\text{eq}}) \quad (15)$$

where $\rho(P')$ is the density of the vapor phase at pressure P' , which is also given by the (inverted) equation of state. The changes in EMLD–DNT, which are needed to account for nonideality, then simply consist of replacing the ideal values of pressure and chemical potential by the more-realistic estimates obtained from the equation of state. In particular, eq 1 must be replaced by

$$\Delta F(n) = \sigma A - \int_0^n \Delta \mu(\rho_v) dn' + \int_0^n v_1(P(\rho_v) - p_{\text{eq}}) dn' \quad (16)$$

where $\rho_v = (N - n)/(V - v_1 n)$ is the density of the vapor phase in the container when a drop that contains n molecules is present, and

$$\Delta \mu(\rho_v) = \int_{P_{\text{eq}}}^{P(\rho_v)} \frac{1}{\rho} \left(\frac{dP}{d\rho} \right) d\rho \quad (17)$$

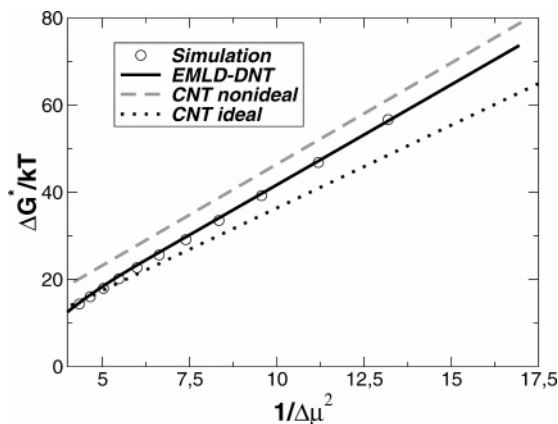


Figure 5. Gibbs free energy of formation of the critical cluster as a function of $1/\Delta\mu^2$ for a truncated and shifted Lennard-Jones fluid ($R_c = 2.5\sigma_{LJ}$) at reduced temperature ($T^* = 0.741$) using the EMLD–DNT model (eq 11, with the Lennard-Jones equation of state; heavy line) and both the ideal (eq 12, dotted line) and nonideal (eq 20, dashed line) versions of CNT. Circles are the data from the simulation of ref 17.

In addition, eq 2 now becomes

$$p(n) = P(\rho_v) + \frac{kT}{(4\pi/3)(R-r)^3} \Theta(n) \quad (18)$$

All remaining equations are the same as those in the ideal case.

We illustrate this situation using a real Lennard-Jones fluid and compare the predictions of the model with the simulation.

Figure 5 plots the results of a recent evaluation of the nucleation barrier in a Lennard-Jones system by a Monte Carlo simulation performed by Ten Wolde and Frenkel.¹⁷ The simulation was performed in the (N, p, T) ensemble and used a truncated (at $R_c = 2.5\sigma_{LJ}$) and shifted Lennard-Jones potential at reduced temperature $T^* = 0.741$. (The reduced temperature is defined as $T^* = kT/u_0$, where u_0 is the characteristic energy of the Lennard-Jones potential. For the case of argon, a reduced temperature of $T^* = 0.741$ would correspond to $T = 88.7$ K.) Under those conditions, the pressure of the supersaturated Lennard-Jones vapor differs significantly from that of the ideal gas. To account for this in the model, instead of the ideal gas values, we used the Lennard-Jones pressure (P_{LJ}) and the chemical potential obtained from the simulated Lennard-Jones equation of state.³³ However, the equation of state reported in ref 33 is for the nontruncated Lennard-Jones fluid. To account properly for the truncation and the shift of the potential at $R_c = 2.5\sigma_{LJ}$, we have corrected the values of the pressure using the equation

$$P = P_{LJ} + \left(\frac{16\pi}{3}\right)\rho^2\left(\frac{1}{R_c^3}\right) \quad (19)$$

as described in ref 34. The values of the (reduced) equilibrium vapor pressure and the (reduced) surface tension used in the EMLD–DNT model were $p_{eq} = 0.00783$ and $\sigma = 0.494$, which are the same values as those used in ref 17.

The results obtained for the height of the nucleation barrier, as a function of $1/\Delta\mu^2$, are plotted in Figure 5 and compared to the results obtained in the simulations. The agreement between the EMLD–DNT and simulation is remarkable, especially for a phenomenon such as nucleation, where severe discrepancies between theoretical predictions and experiment/simulation are common.

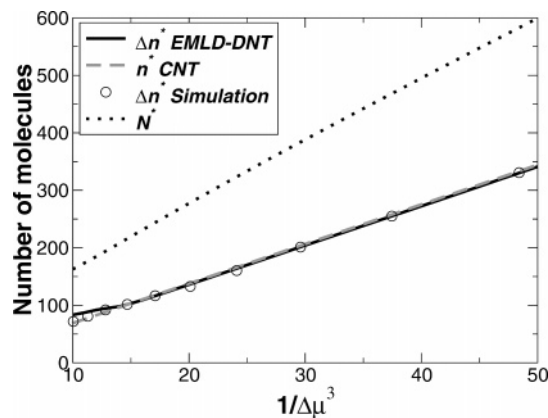


Figure 6. Number of molecules in the critical cluster (Δn^*), as a function of $1/(\Delta\mu)^3$, for a Lennard-Jones fluid at $T^* = 0.741$, as predicted by the nucleation theorem of eq 13 for the EMLD–DNT (heavy line) and by CNT from eq 20 (dashed line), compared to the molecular excess of the critical cluster evaluated in the simulations of ref 17 (open circles). The total number of molecules (N^*) confined in the volume V_{min} used in the construction of the EMLD–DNT cluster is also plotted (dotted line).

For comparison, the heights of the barriers predicted by the nonideal version of CNT,

$$\Delta G_{CNT}^* = \frac{16\pi}{3} \left(\frac{v_1^2 \sigma^3}{\Delta\mu^2} \right) \quad (20)$$

where the real equation of state is used to evaluate $\Delta\mu$, and by the “ideal” version of CNT (eq 12, which assumes that the vapor is ideal) are also plotted in Figure 5. Notice that the assumption of ideality is not good enough in this case.

It is also worth remarking that, as already noted in ref 17, both the simulation results and the prediction of EMLD–DNT are shifted, with respect to CNT, by an almost-constant offset, agreeing with the predictions of scaling theory.

In Figure 6, the molecular excess of the critical nucleus (Δn^*) from the simulations of ref 17, and the predictions of CNT and EMLD–DNT, are plotted as functions of $1/\Delta\mu^3$ for a Lennard-Jones fluid at $T^* = 0.741$. The agreement between the model, simulation, and CNT is excellent, in accordance with the expectations of scaling. Also, the diffuse nature of the EMLD–DNT cluster is demonstrated by the difference between Δn^* and the actual number of molecules inside the volume V_{min} .

However, we note a small discrepancy in the results at high supersaturations. The origin of this discrepancy is probably due to the inability of the simulated equation of state of the Lennard-Jones fluid to represent the properties of very small systems. It is well-known that the properties of small systems can be different from those of the bulk. In particular, it is possible to supersaturate a small portion of a Lennard-Jones fluid beyond what would be possible for the bulk. The simulated equation of state of ref 33 was developed in the thermodynamic limit and, thus, cannot be accurately applied to represent the properties of very small systems. In fact, we have verified the dependence of the properties of the Lennard-Jones vapor—in particular, its pressure—on the size of the system. For example, Figure 7 compares the results of pressure–density isotherms obtained by simulating a nontruncated Lennard-Jones fluid, using different total numbers of particles, with the macroscopic equation of state (labeled “EOS” in the figure). Notice that, contrary to the common situation, where finite size effects are undesirable, here what we need are the properties of a small system and, in

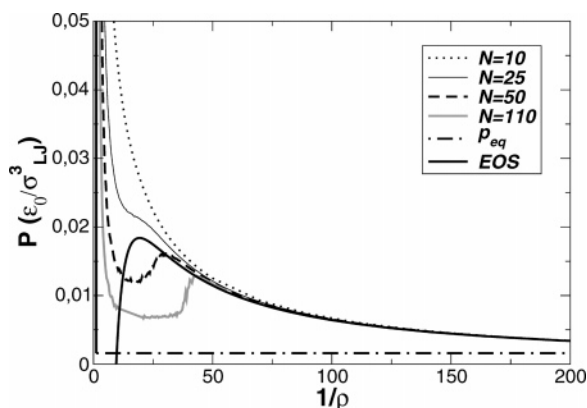


Figure 7. Pressure–density (P – ρ) isotherms for a (nontruncated) Lennard-Jones argon at $T = 85$ K and different values of the total number of molecules. The dotted-dashed line indicates the value of the equilibrium vapor pressure, and the continuous line (labeled “EOS” in the figure) represents the value of the pressure provided by the LJ simulated equation of state of ref 33.

particular, the pressure of a small number of supersaturated LJ molecules, rather than those of the macroscopic system.

The lack of availability of accurate equations of state in the supersaturated regime, and for very small systems, might complicate the application of these methods to real fluids, at least for values of the saturation ratio S close to the spinodal.

6. Temperature Dependence of Nucleation Rates

The height of the nucleation barrier predicted by the EMLD–DNT can be used as an input in the evaluation of nucleation rates. In the classical approach, the nucleation rate is given by the following expression:⁶

$$J = K \exp\left(-\frac{\Delta G^*}{kT}\right) \quad (21)$$

where K is a kinetic pre-exponential factor that is dependent on the rate of addition of molecules to the critical cluster, the total number of molecules, and the curvature of the nucleation barrier around its maximum.

It is worth recalling that this formula is only valid for sufficiently high barriers and it may become a bad approximation close to the spinodal.

Experiments have determined that CNT is not able to correctly predict the dependence of nucleation rate on temperature. Typically, the predictions of CNT for nucleation rates are too low at low temperatures and too high at high temperatures, as it has been observed, for instance, in experiments on *n*-nonane,^{35,36} *n*-alcohols,³⁷ *n*-octane,³⁸ long-chain *n*-alkanes,³⁹ water,⁴⁰ and argon.⁴¹ Thus, it becomes important to evaluate the temperature dependence of nucleation rates predicted by EMLD–DNT, to determine whether the theory is able to remedy this problem.

To investigate temperature dependence in EMLD–DNT, we have evaluated, for temperatures in the range of 55–130 K, the corresponding values of supersaturation that would give a height of the nucleation barrier equal to $\Delta G_{\text{EMLD-DNT}}^* = 25kT$. The values of supersaturation, corresponding to each temperature, were then used in eq 12 to evaluate the height of the barrier predicted by the standard version of CNT, which assumes that the vapor behaves ideally. (Equation 12 is the expression commonly used in the analysis of experiments. For example, it was used in the recent evaluation of nucleation rates of argon.⁴²) The ratio $\exp[-(\Delta G_{\text{EMLD-DNT}}^* - \Delta G_{\text{CNT}}^*)/k_B T]$ then provides a

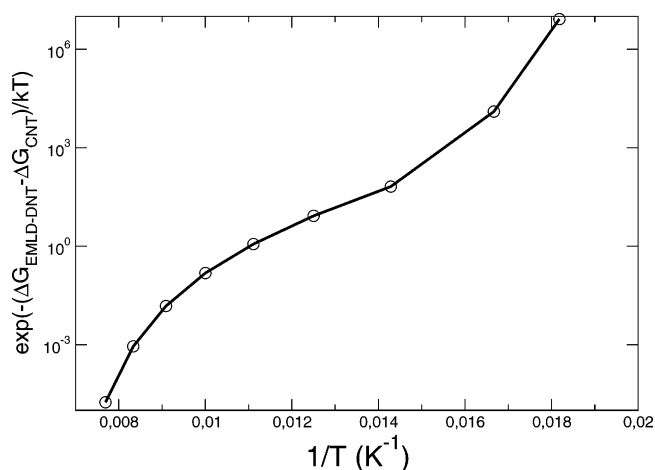


Figure 8. Ratio of the activation factor for EMLD–DNT and CNT, as a function of the inverse of temperature, for Lennard-Jones argon, corresponding to a fixed value of $\Delta G_{\text{EMLD-DNT}}^* = 25k_B T$.

reasonable estimate of the ratio $J_{\text{EMLD-DNT}}/J_{\text{CNT}}$, if we ignore the temperature variation of the prefactor K (which might be significant, especially close to the spinodal). This ratio is plotted in Figure 8 versus $1/T$ for Lennard-Jones argon. In that plot, the simulated equation of state of the (untruncated) Lennard-Jones³³ fluid was used to evaluate the equilibrium density, vapor pressure, and chemical potential of the vapor that appear in the EMLD–DNT model. However, rather than a simulated value of surface tension, we have used an experimental value.⁴² This was done in an attempt to imitate the properties of real argon, which is required for comparison with the experiment. A fully consistent calculation would require both the experimental value of surface tension and the experimental equation of state of real argon.

The rates predicted by EMLD–DNT, and plotted in Figure 8 for argon, show the same qualitative dependence on temperature as the preliminary experimental results by Iland.⁴² The value of the nucleation rate predicted by EMLD–DNT is significantly higher than that predicted by CNT at low temperatures and becomes lower than that predicted by CNT at high temperatures. Similar deviations, with respect to CNT, have been observed experimentally in many substances, as reported in refs 35–41.

A priori, the incorporation of fluctuations in the EMLD–DNT model would seem to lead to nucleation barrier heights that are consistently lower than the classical prediction. Consequently, one would expect that the predictions for nucleation rates by EMLD–DNT should be always higher than those predicted by CNT, for all values of temperature. However, the nonideal nature of the vapor seems to invalidate such a sweeping conclusion.

Figure 9 shows the height of the nucleation barrier predicted by CNT (heavy line and circles), by eq 12 (which assumes that the gas is ideal), and by eq 20 (which uses the Lennard-Jones equation of state (gray line and squares), corresponding to a fixed value of the EMLD–DNT barrier of $25kT$). The EMLD–DNT barrier is always lower than that predicted using eq 20 (the “nonideal” CNT), but it can be higher or lower than the ideal CNT barrier. In fact, it is lower than CNT at low temperatures and higher than CNT at high temperatures. Notice also that the ideal and “nonideal” CNT barriers are very similar at low temperature, but that the ideal result becomes significantly lower at high temperature. Therefore, the nonideal nature of the Lennard-Jones vapor seems to become more important (at

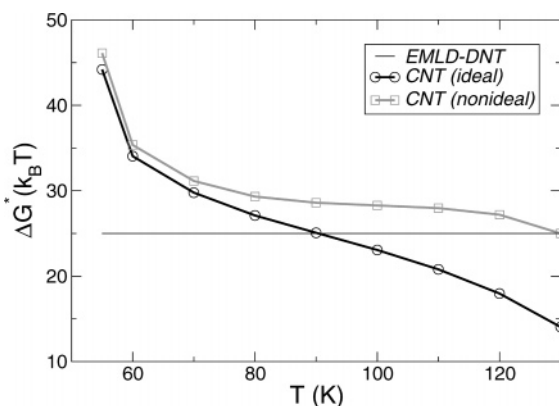


Figure 9. Comparison of the height of the nucleation barrier for argon predicted by ideal CNT (eq 12, heavy line and circles), and nonideal CNT (using the equation of state of the LJ; gray line and squares), as a function of temperature, corresponding to a value of $\Delta G_{\text{EMLD-DNT}}^* = 25k_B T$.

least for the quantities relevant to nucleation) at high temperatures rather than at low temperatures.

In summary, the temperature dependence of the nucleation rates predicted by EMLD–DNT seems to follow the trends observed experimentally. However, to be able to perform a reliable comparison of these predictions with experiment, the experimental equation of state of argon would be required. In addition, an accurate expression for the prefactor K would be helpful.

7. Critical Discussion of the EMLD–DNT Theory

Despite the remarkable properties of the EMLD–DNT and the excellent agreement achieved, with respect to simulation, it is useful to re-examine some of the approximations and assumptions involved in the theory. The excellent agreement with experiment is positive and encouraging, but there is still some room for improvement and it includes some of the following approximations:

(1) The evaluation of the Helmholtz free energy by EMLD–DNT involves some approximations. One is the explicit consideration of the formation of only one drop inside the container. For volumes in the vicinity of the liquid–vapor transition, fluctuations are very strong, and the possibility of having more than one cluster inside the system becomes important. This is one of the reasons for the simulated isotherms being typically smoother than those predicted by theory. In principle, multiple drops can be examined in the manner sketched in ref 14, and the progressive consideration of larger numbers of drops would lead to an improvement of prediction, but only at the expense of significantly complicating the calculation. Deep in the transition region, ignoring the existence of multiple drops could be a problem. However, in EMLD–DNT, the only point of interest is the onset of evaporation, and, at this point, the drop is stable enough to favor the formation of only a single one, in comparison to an entropically favored shattering into many small clusters. Thus, it is expected that shattering does not affect the predictions for intermediate or large clusters, although it might affect smaller clusters close to the spinodal.

(2) In EMLD, curvature corrections to surface tension, which are expected to be relevant for very small systems, were not included, in the interest of simplicity. For Lennard-Jones fluids, the Tolman length is quite small,¹⁷ which suggests, in this case, that these corrections are not too relevant. For other substances,

the correction might be more significant but could be incorporated into the EMLD–DNT cluster.

(3) The contribution of translation is not included in the free-energy estimate of eq 1. Although the incorporation of translation is an essential ingredient in the EMLD isotherms, as a simplifying approximation, it is not included in the expression for the free energy. (Parenthetically, translation is only important at small cluster volumes, such that $r \approx R$ (see eq 23 below).) This point was already noted in ref 14. There is a way to incorporate the effect of translation self-consistently, but it complicates the formalism. In EMLD, the effects of translation are taken into consideration by the contribution of the pressure due to the drop, which is modeled as a single ideal gas molecule. The use of this approximation was justified theoretically in ref 20 and seems to work extremely well, compared to simulations. A self-consistent method of incorporation of the effect of translation on the pressure into the free energy would involve the following thermodynamic integration:

$$\Delta F_{\text{tot}} = - \int p(n) dV = \Delta F(n) - \int p_{\text{drop}} dV \quad (22)$$

The integral $-\int p_{\text{drop}} dV$ yields a translational correction to the free energy of the form

$$\Delta F_{\text{trans}} = k_B T \ln \left(\frac{V}{V_c} \right) + 6k_B T \left(\frac{r}{R-r} \right) + \frac{3}{2} (k_B T) \frac{r^2}{(R-r)^2} \quad (23)$$

where $V_c = (4\pi/3)(R-r)^3$. Curiously, these corrections bear a close resemblance to the “curvature” corrections to surface tension.⁴³ We have verified that the net effect of the incorporation of such corrections is similar to, and seems equivalent to, the use of a larger value of surface tension.

(4) As we have already noted, in the original DNT, the kinetic criterion for selecting the volume was slightly different from that used in the EMLD–DNT model. In the original formulation of DNT, the volume was obtained through a minimization of eq 7, rather than from the minimum of the pressure. Different values of the volume of the cluster could also possibly arise through minimization of other quantities in the variational formulation of transition-state theory. Fortunately, neither the volume nor the properties of the cluster change dramatically upon the election of a slightly different criterion of minimization.

(5) We neglected any possible interaction between the EMLD–DNT cluster and the vapor outside of it. Note that, because of the diffuse character of the cluster, interaction is considered between the vapor and the liquid core inside the volume V . We have seen that the EMLD–DNT cluster contains a significant number of vaporlike molecules, and, in particular, the density at the boundaries of the cluster is expected to be vaporlike. Therefore, if this cluster is immersed in a vapor environment, one would not expect any additional significant interaction between the vapor inside with that outside. Thus, this assumption is not expected to be very restrictive.

The EMLD–DNT theory is designed to be a *simple* extension of the spirit of CNT. For this reason, many of the approximations enumerated in the previous discussion are retained, although they could be removed with relative ease. However, a substantial increase in the level of complexity would not be compensated by the improvement of the results. Future work can account for them consistently.

8. Concluding Remarks

In summary, we have presented a new phenomenological model for nucleation, the “extended modified liquid drop”–

dynamical nucleation theory (EMLD–DNT) model, that shares the same ingredients and simplicity of “classical nucleation theory” (CNT); however, by properly accounting for translational corrections and other fluctuations important at the nanoscale, EMLD–DNT is able to reproduce the spinodal. We have shown that the EMLD–DNT cluster is both thermodynamically and kinetically consistent, and that the predictions of the theory agree remarkably well with both simulation and scaling. A very important feature is the strengthening of the connection between the thermodynamic and nonequilibrium kinetic approach to nucleation, which is already initiated by DNT. Indeed, the symbiosis between the two approaches leads to a nonarbitrary definition of cluster volume, as well as a simple method for evaluating that volume. In these connections, the importance of allowing the “process” to define the cluster is demonstrated.

The simplicity and consistency of EMLD–DNT offers the promise of providing simple yet accurate predictions of nucleation rates for other substances. The revised predictions for nucleation rates provided by the theory may have important impact on a broad diversity of fields, especially in the material and atmospheric sciences.

Acknowledgment. This work has been supported by the National Science Foundation (under NSF Grant No. CHE-03013563). D.R. acknowledges support by the Ministerio de Ciencia y Tecnología of Spain (through the “Ramón y Cajal” Program). We thank P. R. Ten Wolde for sending us his simulation data.

Appendix: Proof of Equation 9

Equation 9 was derived by Lee et al. in an important paper.³⁰ However, the focus of these authors was not on nucleation, but rather on the theory of spherical interfaces. The derivation of eq 9 in ref 30 involved the theory of a capillary drop in a volume V . However, it is important to bear in mind the distinction between a consideration of the drop as a cluster (as in CNT) and the *entire system* as a cluster. For our purposes, we need a more-general derivation that is based only on the thermodynamics of a one-component system of N molecules in V , independent of whether a drop forms or not. We present such a general derivation in this section.

We are interested in the reversible work of formation of one state (the “cluster”, state 2), which is characterized by the presence of an inhomogeneous density profile, starting from another state (a homogeneous vapor, state 1), exhibiting a uniform internal density. The reversible work performed on a system along a particular thermodynamic path is always equal to the increase of the thermodynamic potential characteristic of that path.⁴⁴ Thus, for an (N,p,T) path, the work is given by the increase in Gibbs free energy G along that path $(\Delta G_{N,p,T})$. Similarly, the work performed in the constant (μ,V,T) or constant (N,V,T) process would be given by the change in the grand potential Ω $(\Delta\Omega_{\mu,V,T})$ or the change in the Helmholtz free energy F $(\Delta F_{N,V,T})$ of the system.

We will use the notation 1 and 2, 1' and 2', and 1'' and 2'' for the initial and final states obtained following a path of constant (N,p,T) , (μ,V,T) , and (N,V,T) , respectively. States 2, 2', and 2'', in the presence of the constraining field, can be chosen to be identical, by adjusting properly the values of μ , N , V , and p in the different systems. Note that μ and p are applied outside of the systems and that $\mu = \mu(p,T)$ and $p = p(\mu,T)$. Note also that the initial states would not have to be (and generally will not be) the same; they must only allow the

same final states to be reached via the respective (N,p,T) , (μ,V,T) , and (N,V,T) processes.

As a first step, it is convenient to list several well-known relations among some thermodynamic potentials and associated variables. The Helmholtz free energy is defined as $F = U - TS$, where U is the internal energy and S is the entropy. The Gibbs free energy is $G = F + pV = U - TS + pV$. In a *uniform* system,

$$G = N\mu \quad (\text{A1})$$

The grand potential is given by

$$\Omega = F - N\mu \quad (\text{A2})$$

and, in a uniform system, it can be shown that

$$\Omega = -pV \quad (\text{A3})$$

Retaining the subscripts 1 and 2 for the initial and final states, respectively, we can express $G_2(N,p,T)$ as

$$\begin{aligned} G_2(N,p,T) &= F_2(N,p,T) + pV_2 \\ &= [F_2(N,p,T) - \mu N_2] - [-pV_2] + \mu N_2 \\ &= [F_2(\mu,V,T) - \mu N] - [-pV_1] + \mu N \\ &= \Omega_2(\mu,V,T) - \Omega_1(\mu,V,T) + \mu N \\ &= (\Delta\Omega)_{\mu,V,T} + \mu N \\ &= (\Delta\Omega)_{\mu,V,T} + G_1(N,p,T) \end{aligned} \quad (\text{A4})$$

The various transformations in this equation can be best understood by first recalling that, along a path of constant (μ,T) , the intensive variables (p,T) are also constant. Thus, to ensure that the final states, states 2 and 2', are identical (which is an assumption made in eq A4), one need only adjust an extensive variable (for example, V .) Thus, although the initial states 1 and 1' need not be the same, clearly one could easily choose $N_1 = N$ so that it would equal N_2 , corresponding to μ in state 2', and then simply change V_1 to $V_2 = V_2'$, so that state 2 matched state 2'. Because the *intensive* variables in both processes are essentially constant and equal, there is no difficulty in selecting V_1 and state 1 so that a state 2 identical to state 2' can be accessed from state 1.

Turning to the transformations in eq A4 themselves, the step in the first line merely adds and subtracts μN_2 , and V_2 is identified with V_2' , because the final states are identical. In the second line, $N_2' = N_2$ is simply identified with N being held constant in the (N,p,T) system and V_2' is set equal to V_1' , because $V_2' = V_1' = V$ in the (μ,V,T) process.

Furthermore, in the second line, the arguments of F_2 are changed from (N,p,T) to (μ,V,T) , because, as we have explained, both sets of arguments correspond to the same state. In the third line, the quantities in brackets in the second line are converted to Ω values. The first set of brackets simply contains the definition of Ω in state 2', whereas the second set of brackets contains the definition of Ω in the uniform state 1', where p , similar to that observed for μ , is the same in both states 1 and 1'. The transformation in the fourth line is obvious, and, in the fifth line, μN is identified as $G_1(N,p,T)$, because the density distribution in state 1 is uniform.

Rearranging eq A4 yields

$$(\Delta\Omega)_{\mu,V,T} = G_2(N,p,T) - G_1(N,p,T) = (\Delta G)_{N,p,T} \quad (\text{A5})$$

which shows that, when μ is determined by the necessary

thermodynamic relation ($\mu = \mu(p, T)$), the work of formation of the final inhomogeneous state, at constant p , starting from an appropriate uniform initial state, is equal to the work of formation at constant μ , again starting from another appropriate uniform initial state. There is nothing in the proof that requires the final inhomogeneous state to correspond to an extremum of a thermodynamic potential, e.g., to a condensation nucleus.

With eq A5 in hand, we can continue the derivation of eq 9. For the final state $2''$ in a N, V, T process, we can write

$$\Omega_{2''}(\mu, V, T) = \Omega_{2''}(N, V, T) = F_{2''}(N, V, T) - \mu N$$

or

$$F_{2''}(N, V, T) = \Omega_{2''}(N, V, T) + \mu N = \Omega_{2''}(\mu, V, T) + \mu N \quad (\text{A6})$$

In the initial state in the (N, V, T) system, the uniform vapor has the density $\bar{\rho} = N_1/V_1 = N/V$ and the Helmholtz free energy density may be represented by $f(\bar{\rho})$; therefore, the free energy in that state is $f(\bar{\rho})V_1 = f(\bar{\rho})V$. We can now write

$$\begin{aligned} (\Delta F)_{N,V,T} &= F_{2''}(N, V, T) - f(\bar{\rho})V \\ &= [\Omega_{2''}(\mu_{2''}, V, T) + \mu_{2''}N] - f(\bar{\rho})V \\ &= [\Omega_{2''}(\mu, V, T) + p_2V] + \mu_{2''}N - f(\bar{\rho})V - p_2V \\ &= [\Omega_{2''}(\mu, V, T) + p_1V] + \mu_{2''}N - f(\bar{\rho})V - p_2V \\ &= [\Omega_{2''}(\mu, V, T) - \Omega_1(\mu, V, T)] + \mu_{2''}N - f(\bar{\rho})V - p_2V \\ &= (\Delta\Omega)_{\mu,V,T} + \mu_{2''}N - [\mu_1N - p_1V] - p_2V \\ &= (\Delta\Omega)_{\mu,V,T} - N[\mu(\bar{\rho}) - \mu] + V[p(\bar{\rho}) - p] \\ &= (\Delta\Omega)_{\mu,V,T} - N\Delta\mu_0 + V\Delta p \\ &= (\Delta G)_{N,p,T} - N\Delta\mu_0 + V\Delta p \quad (\text{A7}) \end{aligned}$$

where $\Delta\mu_0 = \mu(\bar{\rho}) - \mu$, $\Delta p = p(\bar{\rho}) - p$, and $(\Delta F)_{N,V,T} = F_{2''}(N, V, T) - f(\bar{\rho})V$. The term on the left-hand side of the last line, which is equal to the sum of the three terms on the right-hand side of the last line of this series of equations, constitutes eq 9. The procedure and transformations in eq A7 are similar to those involved in eqs A4 and A5, and the reader might be able to recognize them without too much help. However, a brief explanation, as we now offer, should be helpful.

The second equality in the first line of eq A7 simply involves the substitution of eq 15 (the bracketed quantity). Because of the assumed identity of the final states in the (N, V, T) and (μ, V, T) processes, $\mu_{2''}$ is the same as μ_2 and both are simply the parameter μ of the (μ, V, T) process. Similarly, the arguments of $\Omega_{2''}$ could just as easily be (N, V, T) . The only step in the second line is the addition and subtraction of p_2V , and one should recall that, in the (μ, V, T) process, $p_2 = p_1 = p$, where p is the constant pressure of the (N, p, T) process, and in the third line, the parameter p_2 in the brackets is replaced by its equivalent, p_1 . Now, $-p_1V$ is just the value of the grand potential in the initial uniform system, so that p_1V in the third line is replaced, in the fourth line, by $-\Omega_1(\mu, V, T)$. In the fifth line, $(\Delta\Omega)_{\mu,V,T}$ is the bracketed quantity in the fourth line, and the bracketed quantity in the fifth line is just $f(\bar{\rho})V$ from the preceding line. The term μ_1N is just the Gibbs free energy in the uniform initial state of the (N, V, T) process, and the subtraction of p_1V just leaves the Helmholtz free energy $f(\bar{\rho})V$. The sixth line is a rearrangement

of the fifth line. The seventh line defines the bracketed quantities of the sixth line as $\Delta\mu_0$ and Δp , respectively.

We can differentiate eq A7 to obtain

$$\left[\frac{\partial(\Delta F)_{N,V,T}}{\partial N} \right]_{V,T} = \left[\frac{\partial(\Delta G)_{N,p,T}}{\partial N} \right]_{V,T} - \Delta\mu_0 - N \left[\frac{\partial\Delta\mu_0}{\partial N} \right]_{V,T} + V \left[\frac{\partial\Delta p}{\partial N} \right]_{V,T} \quad (\text{A8})$$

In this equation, the last two terms cancel, because of the Gibbs–Duhem relation. The remaining equation is

$$\left[\frac{\partial(\Delta F)_{N,V,T}}{\partial N} \right]_{V,T} = \left[\frac{\partial(\Delta G)_{N,p,T}}{\partial N} \right]_{V,T} - \Delta\mu_0 \quad (\text{A9})$$

However, the first term on the left-hand side is just the definition of the difference in chemical potentials:

$$\left[\frac{\partial(\Delta F)_{N,V,T}}{\partial N} \right]_{V,T} = \mu_{\text{EMLD–DNT}} - \mu(\bar{\rho}) \quad (\text{A10})$$

where $\mu_{\text{EMLD–DNT}}$ is the chemical potential of the EMLD–DNT cluster. When this chemical potential is equal to the externally imposed chemical potential μ , i.e., when

$$\mu_{\text{EMLD–DNT}} = \mu \quad (\text{A11})$$

then eq A9 implies that

$$\left[\frac{\partial(\Delta G)_{N,p,T}}{\partial N} \right]_{V,T} = 0 \quad (\text{A12})$$

and becomes eq 10 in the body of the text, thus proving that equation. However, eq A12 is just the condition for an extremum (maximum) of $(\Delta G)_{N,p,T}$. Thus, the (N, V) -cluster at this maximum serves as the nucleus for condensation in the constant pressure system. Because it is easier to work with a stable cluster, the (N, V, T) system is the one of choice for both analysis and simulation. However, for nucleation, the process in the (μ, V, T) system is closest to reality. The analytical convenience of the (N, V, T) system thus impels us (i) to evaluate the work of cluster formation by way of $(\Delta F)_{N,V,T}$ in the (N, V, T) system, and (ii) to use the result in eq 9 to evaluate $(\Delta G)_{N,p,T} = (\Delta\Omega)_{\mu,V,T}$, which is the work of formation that we are seeking.

Despite the apparent simplicity of these thermodynamic derivations, there are many subtleties involved. Many of them are related to the specification of what variables are held constant in the corresponding changes of state. Because of the importance of the rigor of these equations in the model, we will try to state and clarify all these subtleties properly in a future work.

References and Notes

- (1) Senger, B.; Schaaf, P.; Corti, D. S.; Bowles, R.; Voegel, J. C.; Reiss, H. *J. Chem. Phys.* **1999**, *110*, 6421, 6438.
- (2) Evans, R. *Adv. Phys.* **1979**, *28*, 143.
- (3) Oxtoby, D. W.; Evans, R. *J. Chem. Phys.* **1988**, *89*, 7521.
- (4) Abraham, F. F. *Homogeneous Nucleation Theory*; Academic Press: New York, 1974.
- (5) Oxtoby, D. W. *J. Phys.: Condens. Matter* **1992**, *4*, 7627.
- (6) Laaksonen, A.; Talanquer, V.; Oxtoby, D. W. *Annu. Rev. Phys. Chem.* **1995**, *46*, 489.
- (7) Fisher, M. E. *Rep. Prog. Phys.* **1967**, *30*, 615; *Physics* **1967**, *3*, 255.
- (8) Dillmann, A.; Meier, G. E. A. *Chem. Phys. Lett.* **1989**, *160*, 71; *J. Chem. Phys.* **1991**, *94*, 3872.
- (9) Kalikmanov, V. I.; van Dongen, M. E. H. *Phys. Rev. E* **1993**, *47*, 3532; *J. Chem. Phys.* **1995**, *103*, 4250.
- (10) Talanquer, V. *J. Chem. Phys.* **1997**, *106*, 9957.
- (11) Kashchiev, D. *J. Chem. Phys.* **2003**, *118*, 1837.

- (12) Schmelzer, J. W. P.; Schmelzer, J.; Gutzow, I. S. *J. Chem. Phys.* **2000**, *112*, 3820.
- (13) Moody, M. P.; Attard, P. *Phys. Rev. Lett.* **2003**, *91*, 056104.
- (14) Reguera, D.; Bowles, R. K.; Djikaev, Y.; Reiss, H. *J. Chem. Phys.* **2003**, *118*, 340.
- (15) Reguera, D.; Reiss, H. *J. Chem. Phys.* **2003**, *119*, 1533.
- (16) Schenter, G. K.; Kathmann, S. M.; Garrett, B. C. *Phys. Rev. Lett.* **1999**, *82*, 3484.
- (17) Ten Wolde, P. R.; Frenkel, D. *J. Chem. Phys.* **1998**, *109*, 9901.
- (18) McGraw, R.; Laaksonen, A. *Phys. Rev. Lett.* **1996**, *76*, 2754.
- (19) Note that our model only considers the presence of one drop in the system, whereas it is possible to have more than one drop inside the volume. In fact, this possibility was contemplated in ref 14, where it was shown that it leads to better agreement between the predictions of the model and the simulations, in the transition region between the drop and the vapor, where the effect of these fluctuations is more important.
- (20) Reiss, H.; Reguera, D. *J. Phys. Chem. B* **2004**, *108*, 6555.
- (21) Weakliem, C. L.; Reiss, H. *J. Chem. Phys.* **1993**, *99*, 5374.
- (22) Reiss, H.; Tabazadeh, A.; Talbot, J. *J. Chem. Phys.* **1990**, *92*, 1266.
- (23) Ellerby, H. M.; Weakliem, C. L.; Reiss, H. *J. Chem. Phys.* **1991**, *95*, 9209.
- (24) Ellerby, H. M.; Reiss, H. *J. Chem. Phys.* **1992**, *97*, 5766.
- (25) Lee, J. K.; Barker, J. A.; Abraham, F. F. *J. Chem. Phys.* **1973**, *58*, 3166; **1974**, *60*, 246.
- (26) Talanquer, V.; Oxtoby, D. W. *J. Chem. Phys.* **1994**, *100*, 5190.
- (27) Reiss, H. *J. Stat. Phys.* **1970**, *2*, 83.
- (28) Schenter, G. K.; Kathmann, S. M.; Garret, B. C. *J. Chem. Phys.* **1999**, *110*, 7951.
- (29) Kathmann, S. M.; Schenter, G. K.; Garrett, B. C. *J. Chem. Phys.* **2002**, *116*, 5046.
- (30) Lee, D. J.; Telo da Gama, M. M.; Gubbins, K. E. *J. Chem. Phys.* **1986**, *85*, 490.
- (31) Bowles, R. K.; Reguera, D.; Djikaev, Y.; Reiss, H. *J. Chem. Phys.* **2001**, *115*, 1853; **2002**, *116*, 2330.
- (32) Kashchiev, D. *J. Chem. Phys.* **1982**, *76*, 5098.
- (33) Johnson, J. K.; Zollweg, J. A.; Gubbins, K. E. *Mol. Phys.* **1993**, *78*, 591.
- (34) Smit, B. *J. Chem. Phys.* **1992**, *96*, 8639.
- (35) Wagner, P. E.; Strey, R. *J. Chem. Phys.* **1984**, *80*, 5266.
- (36) Hung, C. H.; Krasnopol, M. J.; Katz, J. L. *J. Chem. Phys.* **1989**, *90*, 1856.
- (37) Strey, R.; Wagner, P. E.; Schmeling, T. *J. Chem. Phys.* **1986**, *84*, 2325.
- (38) Rudek, M. M.; Fisk, J. A.; Chakarov, V. M.; Katz, J. L. *J. Chem. Phys.* **1996**, *105*, 4707.
- (39) Rusyniak, M.; Abdelsayed, V.; Campbell, J.; El-Shall, M. S. *J. Phys. Chem.* **2001**, *105*, 11866.
- (40) Wölk, J.; Strey, R. *J. Phys. Chem.* **2001**, *105*, 11683.
- (41) Fladerer, A. Ph.D. Thesis, University of Cologne, Cologne, Germany, 2002.
- (42) Iland, K. Ph.D. Thesis. University of Cologne, Cologne, Germany, 2004.
- (43) (a) Tolman, R. C. *J. Chem. Phys.* **1949**, *17*, 333. (b) Rowlinson, J. S.; Widom, B. *Molecular Theory of Capillarity*; Clarendon Press: Oxford, U.K., 1982.
- (44) Reiss, H. *Methods of Thermodynamics*; Dover: New York, 1996.